Development of a Robotic Thumb Rehabilitation System Using a Soft Pneumatic Actuator and a Pneumatic Artificial Muscles-Based Parallel Link Mechanism

Kouki Shiota, Tapio V.J. Tarvainen, Masashi Sekine, Kahori Kita and Wenwei Yu

Abstract The main function of a hand is to grasp and manipulate objects, and the thumb contributes most to this function. However, thumb rehabilitation devices, especially soft robotic gloves, have not been widely investigated. Soft pneumatic actuators are lighter, more flexible, and easier maintenance than other actuators. This makes them safer and more cost-effective. In this paper, we present a design for a soft robotic thumb rehabilitation system. We used a soft pneumatic actuator for bending (SPAB) for flexion-extension motion. For the carpometacarpal (CMC) joint, we used a parallel link mechanism by placing pneumatic artificial muscles (PAM) around it in three directions. We evaluated whether this setup of SPAB and PAM could enable the required three-dimensional thumb motions by using a prototype system on a dummy thumb. The results showed that the proposed mechanism enables opposition, abduction, and adduction motions for the thumb.

Keywords Hand rehabilitation · Soft pneumatic robotics · Power assist

K. Shiota (✉) · T.V.J. Tarvainen (✉)
Graduate School of Engineering, Chiba University, Chiba, Japan
e-mail: acaa2343@chiba-u.jp

T.V.J. Tarvainen
e-mail: tapio.tarvainen@chiba-u.jp

M. Sekine (✉) · K. Kita (✉) · W. Yu (✉)
Center for Frontier Medical Engineering, Chiba University, Chiba, Japan
e-mail: sekine@office.chiba-u.jp

K. Kita
e-mail: kkita@chiba-u.jp

W. Yu
e-mail: yuwill@faculty.chiba-u.jp

W. Chen et al. (eds.), *Intelligent Autonomous Systems 14*,
Advances in Intelligent Systems and Computing 531,
DOI 10.1007/978-3-319-48036-7_38

1 Introduction

In Japan, there are over 1.17 million stroke patients. The most common impairments after stroke are motor deficits, such as hemiparesis, which is experienced by approximately 80 % of stroke survivors [1]. These patients experience either partial or total absence of hand motor function, which can considerably reduce quality of life, because of major restrictions on activities of daily living (ADL) and ability to work.

Rehabilitation is provided under the direction and assistance of an occupational therapists or a physiotherapists, in order to have the patients return to normal life, and to improve their ability to perform ADL adequately. Especially repetitive task practice has been shown to be effective in improving motor function after stroke [2, 3]. However, hand rehabilitation is labor intensive and costly due to the required long hours and terms of training with a therapist. In order to deal with this problem, many robotic hand rehabilitation systems have been investigated recently to automate some of the therapy [2, 4, 5].

In recent years, robotic rehabilitation devices that use soft fluidic actuators with high level of elasticity have been studied [4, 6, 7]. Soft fluidic actuators are light, flexible, and easy maintenance. These properties make them inherently safer, and more cost-effective than many other actuation systems that are based on rigid mechanics. Thus, they would be a good choice for rehabilitation, which requires high level of safety, and relatively low cost, as the goal is to replace human labor.

The main function of a hand is to grasp and manipulate objects, and the thumb contributes most to this function. Losing the thumb causes a 40 % loss of overall hand function [8]. Therefore, the thumb could be considered the most important target in hand rehabilitation. However, because the joints of the thumb make very complicated motions, their control is difficult. Thumb rehabilitation, especially with soft robotic gloves, has not been widely investigated.

In this paper, we present a design for a soft robotic thumb rehabilitation system, using a soft pneumatic actuator and a pneumatic artificial muscle-based parallel link mechanism, with the goal of facilitating research in hand rehabilitation therapy.

2 Methods

2.1 Mechanism Design

The main function of the interphalangeal (IP) and metacarpophalangeal (MP) joint is flexion-extension. Therefore we use a soft pneumatic actuator for bending (SPAB), which is placed on the dorsal side of the thumb. Thus, the palmar side is left free. Furthermore, there is no need for fine adjustment of the joint pivot point, unlike in systems that are based on rigid mechanics, because the actuator shape conforms to the shape of the assisted digit. For the carpometacarpal (CMC) joint,

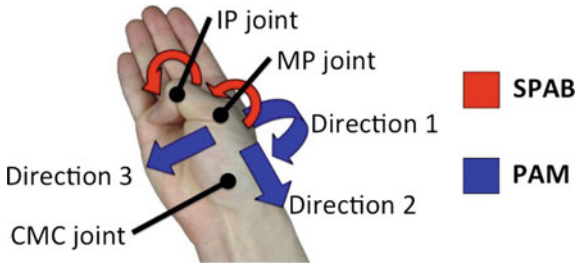

Fig. 1 Functional concept of the mechanism

we used a parallel link mechanism by coupling pneumatic artificial muscles (PAM) in three directions around the proximal side of the MP joint (Fig. 1). This simple mechanism enables, ideally, a full stable control and a wide range of motion for the first metacarpal bone. In consideration of comparing the amount of actuator contraction and muscle contraction, we use two PAMs for each direction. We defined traction directions 1: dorsal side, 2: radial side, 3: palmar side (Fig. 1).

2.2 System Concept

The proposed system layout is shown in Fig. 2. The PAMs are placed on an orthotic structure on the forearm to take their size and contraction motion range into consideration. The motion is transmitted to the thumb through wires that are guided by hard tubing attached to the orthosis.

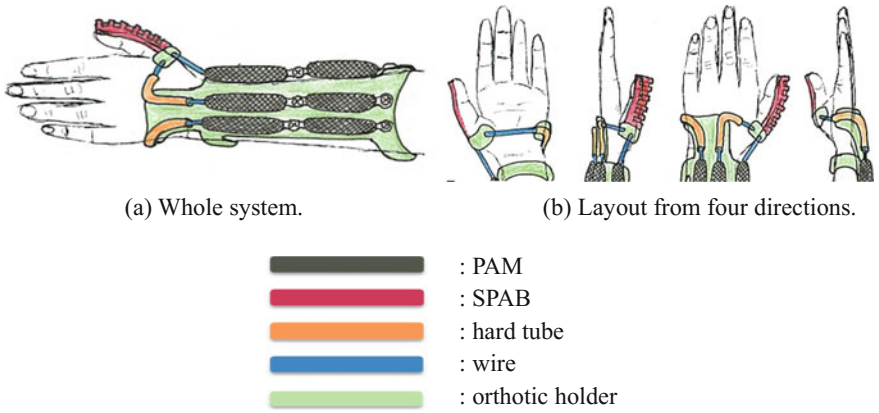

(a) Whole system. (b) Layout from four directions.

Fig. 2 System concept

2.3 Pneumatic Artificial Muscle (PAM)

We used PM-10P (SQUSE Co.) as PAM (Fig. 3). Its specification is shown in Table 1.

2.4 Soft Pneumatic Actuator for Bending (SPAB)

For the thumb flexion we used a 2-pocket SPAB (Fig. 4) [10], which is a modified version of similar actuators by Deimel and Brock [11]. The actuator's specification is shown in Table 2.

Fig. 3 External appearance of PAM

Table 1 Specification of PM-10P [9]

Drive system	McKibben type
Average maximum contraction	30 %
Maximum traction (at rated pressure)	100 N
Specification fluid	Air
Rated pressure	200 kPa
Mass	3 g
Maximum pressure (range of use)	250 kPa
Durability (inflation cycles at rated pressure)	50,000
External dimensions (no pressure) (full length × outer diameter)	75 × φ10 mm
External dimensions (pressurized)	52.5 × φ24 mm

(a) Unpressurized (b) Pressurized

Fig. 4 External appearance of SPAB

Table 2 Specification of SPAB

Rated pressure		150 kPa
Specification fluid		Air
Material	Main body	Silicone
	Reinforcement fiber	Cotton thread
	Inextensible bottom layer	Polypropylene net
Mass		27 g
External dimensions		W18 × H17 × L105 mm

2.5 Prototype

We evaluated the proposed mechanism using a prototype (Fig. 5a, b). A supporting structure for the system was made from wood, and fixed to a desk. A first metacarpal bone holder was made of polymer clay and a PAM holder was made from wood (Fig. 5c). We used a Velcro straps for the fixation of PAM and the first metacarpal bone holder. Total weight of the prototype system was approximately 100 g, without an orthotic holder, and excluding the dummy hand structure and its supports.

2.6 Thumb Dummy Hand

For the measurement of the prototype, we made a thumb dummy hand in imitation of a human thumb (Fig. 6). For the CMC joint we used a plastic ball joint, which enabled flexion-extension and adduction-abduction. The part equal to the first metacarpal and phalanx bones were made of 5 mm diameter wood sticks. The sticks were covered with hot melt glue to form the general shape of the bones.

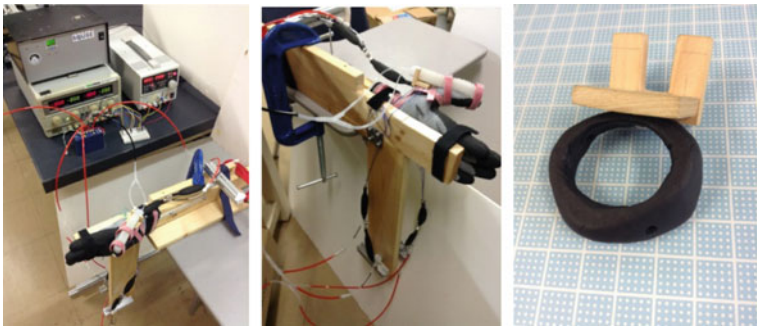

(a) View of palmar side. (b) View of dorsal side (c) First metacarpal bone holder (10.5 g)

Fig. 5 Prototype and first metacarpal bone holder

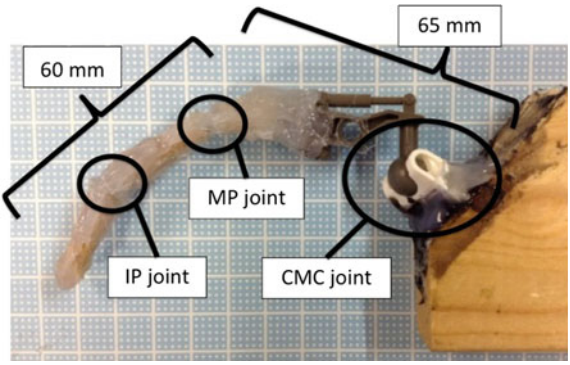

Fig. 6 Thumb structure for dummy hand

The IP and MP joints were made as flexural joints from the same hot melt glue to enable only flexion-extension. The length of the metacarpal part was 65 mm, and the combined length of phalanges was 60 mm. These measures were based on the data of Kawauchi [12].

2.7 Measurement of SPAB

The following experiments were carried out to confirm whether the modified SPAB for thumb satisfied the requirements for using it for motion assist.

To estimate the trajectory of the thumb tip, the SPAB was pressurized with air three times while the camera captured the motion from the side. For this, the SPAB was clamped in a vertical position from its proximal end, and a black marker was used to mark the tip, the middle point, and the proximal end. The pressure inside the SPAB was gradually increased from 0 to 150 kPa, in increments of 25 kPa. The SPAB tip angle was measured from the images as the angle between the vector formed by the proximal end and tip markers at 0 kPa, and the tip normal vector at different pressures.

A force gauge (ZTS-i, IMADA Co.) was used to measure the force output. It was brought in contact with the tip of the actuator as shown in Fig. 7. The pressure inside the SPAB was gradually increased from 0 to 125 kPa, in increments of 25 kPa, and the force exerted by its tip was recorded. The rated pressure was 150 kPa, but it was not considered, because the tip of the SPAB did not stay on the pedestal of the force gauge due to its large deformation at 150 kPa. The experiment was repeated three times.

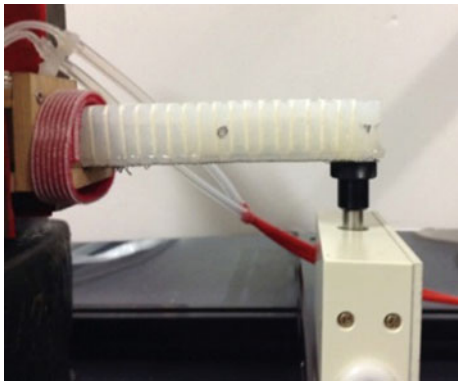

Fig. 7 View of force measurement setup

2.8 Thumb Opposition Movement

Support of the thumb opposition movement is one of the most important functions for a hand rehabilitation device. We evaluated whether the proposed mechanism could really assist opposition. At first, 200 kPa air pressures was applied to dorsal and radial side PAMs. Next, the air pressure was released from them, and 200 kPa air pressure was applied to the palmar side PAM. In the end, 150 kPa air pressure was applied to the SPAB.

2.9 Angle of Thumb Opposition

The overall motion path of the thumb during opposition is combination of abduction, medial rotation, and flexion. However, in this study we defined the angle of thumb opposition as the angle between a vector from the index finger tip to the thumb tip, and the back board, which was parallel to the back of the dummy hand (Fig. 8).

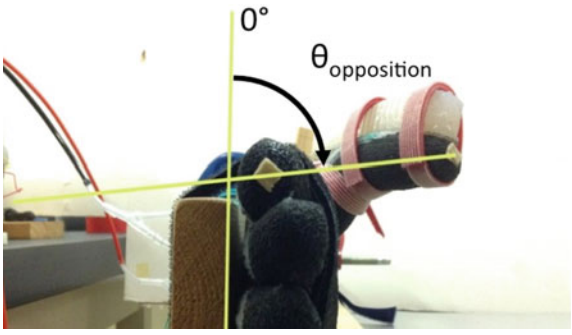

Fig. 8 Angle of thumb opposition

PAM2 (radial side) pressure was kept constant, while PAM1 (dorsal side) and PAM3 (palmar side) pressures were changed in 50 kPa increments from 200 to 0 kPa, and from 0 to 200 kPa, respectively. This was repeated five times, increasing PAM2 pressure from 0 to 200 kPa, in 50 kPa increments. From the results we calculated the relationship between pressure and angle of thumb opposition. We considered the target value to be 60°, based on the results of Li and Tang [13].

2.10 Angle of Adduction-Abduction

The wide range of motion of the CMC joint enables the thumb opposition and adduction-abduction motions [14]. Many activities of everyday life require these two complex motions. Yonemoto et al. defined the angle of thumb adduction-abduction as 60° [15]. We measured the angle using this value as a reference. We put two markers on the side of the first metacarpal bone, one on the index finger tip, and one approximately where the end of the radial bone would be. We defined the angle of thumb abduction ($\Psi_{abduction}$) and adduction ($\varphi_{adduction}$) as the angle between these markers (Fig. 9). The pressure of each PAM was gradually changed from 0 to 200 kPa, in increments of 50 kPa. We calculated the relationship between the pressure and the angle of thumb adduction and abduction. The experiment was repeated three times.

3 Results

3.1 Measurement of SPAB

Results of trajectory measurements are shown in (Fig. 10a, b. Error bars show the standard deviations. The mean maximum bending angle was 296° at 150 kPa pressure.

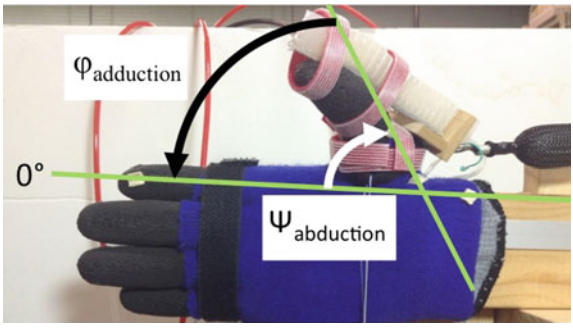

Fig. 9 Angle of adduction-abduction

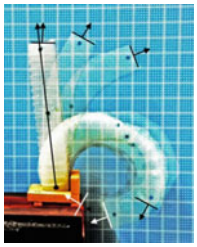

(a) Trajectory of the SPAB tip.

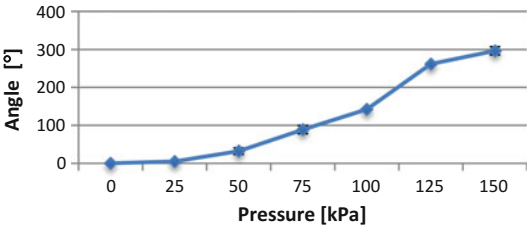

(b) Mean bending angle.

Fig. 10 Results of the trajectory and bending angle

Fig. 11 The mean tip force data of the SPAB with standard deviations

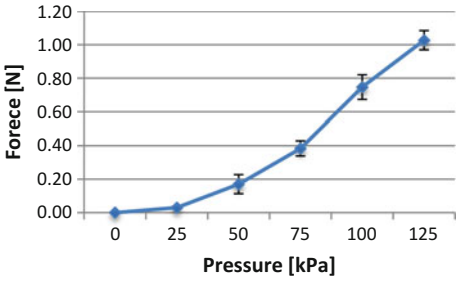

The mean force result is shown in Fig. 11. The mean maximum tip force at 125 kPa was 1.03 N.

3.2 *Thumb Opposition Movement*

Figure 12 shows the states of movements. The proposed mechanism was able to achieve the needed motions to assist opposition.

3.3 *Angle of Thumb Opposition*

The result is shown in Fig. 13, Table 3. We labeled the results from *a* to *e* based on PAM2 pressure increments. On the whole, the mean maximum angle difference was 69.7° between *c*-*i* and *a*-*v*.

Front view			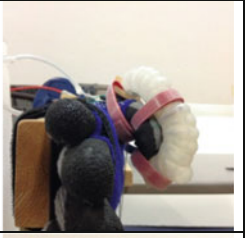
Side view			
	Pressure was applied to activate PAM1 and PAM2.	Pressure was released from PAM1 and PAM2, and PAM3 was activated.	Pressure was applied to activate SPAB.

Fig. 12 Thumb opposition movement

3.4 Angle of Adduction and Abduction

The result is shown in Fig. 14. In adduction, the mean maximum angle was 62.7° at f-i, the mean minimum angle was 3.3° at f-v, and their difference was 59.3°. Similarly, in abduction, the mean maximum angle was 57.3° at f-i, the mean minimum angle was 3.3° at f-v, and their difference was 54.0°.

4 Discussion

4.1 Measurement of SPAB

Regarding the bending angle, the combined range of motion of IP and MP joint is 160° as described by Yonemoto et al. [15]. Experiment results from tracking the tip of the SPAB demonstrate its ability to curl approximately 300°. The result of the SPAB tip force is almost the same as in a previous study by Polygerinos et al. [7]. The mean maximum bending angle and force of their actuator were 320° and 1.21 N. Based on this, we can say that the SPAB has good enough performance for assisting the flexion-extension movement.

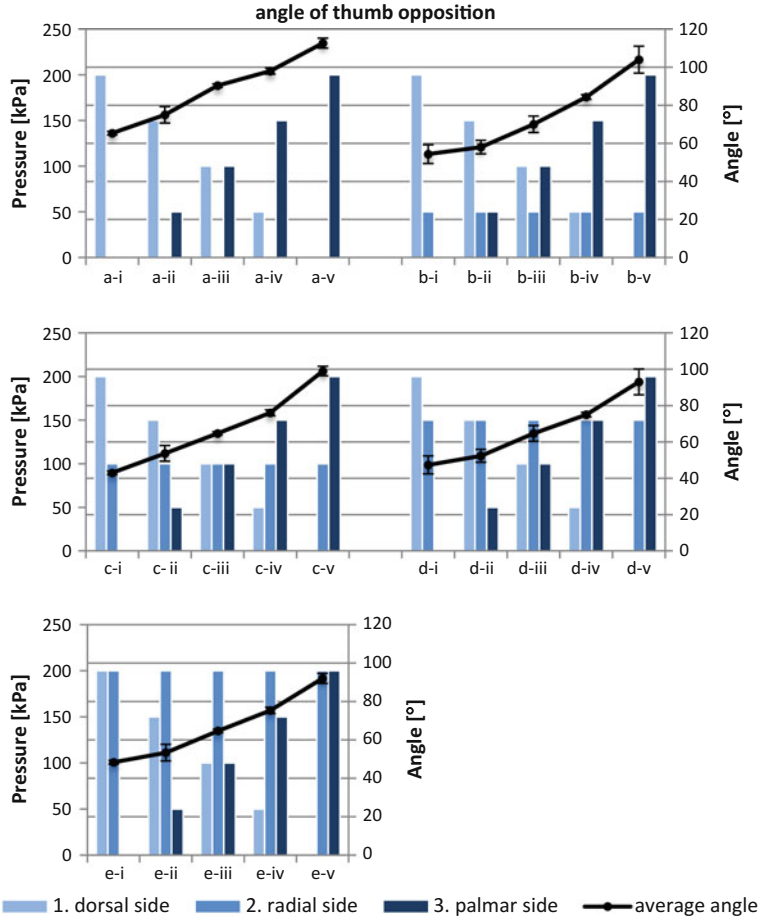

Fig. 13 The results of angle of thumb opposition. The *vertical axes* show the pressure and angle and the *horizontal axis* shows alteration of each PAM air pressure. *Bar graphs* show each PAM air pressure and the *line graph* shows average angles. *Error bars* show the standard deviations

Table 3 Mean minimum and maximum angle of each PAM2 pressure

PAM2 (radial side) pressure (kPa)	Minimum (°)	Maximum (°)	Difference (°)
0 (a)	65.3	112.7	47.4
50 (b)	54.3	104.0	49.7
100 (c)	43.0	99.0	56.0
150 (d)	47.3	93.0	45.7
200 (e)	48.3	92.0	43.7

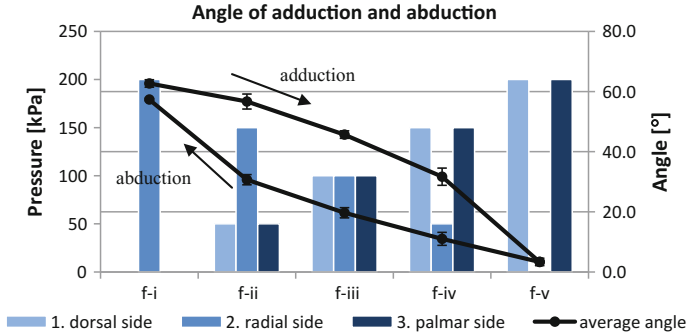

Fig. 14 The results of angle of adduction and abduction. The *vertical axis* shows the pressure and angle and the *horizontal axis* shows alteration of each PAM air pressure. *Bar graphs* show each PAM air pressure and the *line graph* shows average angles. *Error bars* show the standard deviations

4.2 Thumb Opposition Movement

The proposed mechanism enables opposition that is the most important motion of the thumb, and it could assist CMC, IP, and MP joints independently.

4.3 Angle of Thumb Opposition, Adduction and Abduction

The adduction, abduction and opposition are possible with the proposed mechanism, and the adjustment of the angle is possible by changing pressure independently for each actuator. However, there were standard deviations of more than 7° at *b*-*v* and *c*-*v*, as seen in Fig. 13. Also, hysteresis in the actuator response between adduction and abduction, as shown in Fig. 14, caused the intermediate state angle to be different. This could cause unwanted stress on the user's joints, and should be considered in the future to ensure stable and safe movement assist.

Our future prospects are making of a geometric model and a controller based on it, examining the use of the system on a real human hand, and improving its portability. After this, we will develop a device that assists all digits, and verify its efficacy for rehabilitation.

5 Conclusion

In this paper, we presented a design for a soft robotic thumb rehabilitation system, using a parallel link mechanism with pneumatic actuators. We evaluated the proposed mechanism using a prototype. The results showed that the proposed mechanism enables opposition, radial abduction, and ulnar adduction motions for the thumb.

References

1. The Royal College of Physicians Intercollegiate Stroke Working Party: National clinical guideline for stroke. 4th edn. London: Royal College of Physicians (2008)
2. Kutner, N.G., Zhang, R., Butler, A.J., Wolf, S.L., Alberts, J.L.: Quality-of-life change associated with robotic-assisted therapy to improve hand motor function in patients with subacute stroke: a randomized clinical trial. Phys. Ther. **90**(4), 807–824 (2012)
3. Wolf,, S.L., Blanton, S., Baer, H., Breshears, J., Butler, A.J.: Repetitive task practice: a critical review of constraint-induced movement therapy in stroke. Neurol **8**(6), 325–338 (2002). PMC. Web. 1 Mar. 2016 http://doi.org/10.1097/01.nrl.0000031014.85777.76
4. Heo, P., Gu, G.M., Lee, S., Rhee, K., Kim, J.: Current hand exoskeleton technologies for rehabilitation and assistive engineering. Int. J. Precis. Eng. Manuf. **13**(5), 807–824 (2012)
5. Takahashi, C.D., Der-Yeghiaian, L., Le, V., Motiwala, R.R., Cramer, S.C.: Robot-based hand motor therapy after stroke. Brain **131**(2), 425–437 (2008)
6. Noritsugu, T., Yamamoto, H., Sasaki, D., Takaiwa, M.: Wearable power assist device for hand grasping using pneumatic artificial rubber muscle. In: SICE Annual Conference (Hokkaido Institute of Technology, Japan), pp. 420–425. SICE 1999, Aug 2004
7. Polygerinos, P., Wang, Z., Galloway, K.C., Wood, R.J., Walsh, C.J.: Soft robotic glove for combined assistance and at-home rehabilitation. Robot Auton Syst **73**, 135–143 (2015). doi:10.1016/j.robot.2014.08.014
8. Jones, L.A., Lederman, S.J.: Human Hand Function. Oxford University Press, New York (2006)
9. SQUSE, PM-10P, (http://www.squse.co.jp/product/detail.php?id=9) (in Japanese), Accessed 7 June 2016
10. Tarvainen, T.V.J., Yu, W.: Preliminary results on multi-pocket pneumatic elastomer actuators for human-robot interface in hand rehabilitation. In: IEEE-ROBIO, 6−9 Dec 2015
11. Deimel, R., Brock, O.: A compliant hand based on a novel pneumatic actuator. In: Proceedings of IEEE International Conference on Robotics and Automation (ICRA) (2013)
12. Kawauchi, M.: AIST dimensions data of the Japanese hand (2012). (https://www.dh.aist.go.jp/database/hand/index.html) (in Japanese), Accessed 7 June 2016
13. Li, Z.M., Tang, J.: Coordination of thumb joints during opposition. J. Biomech. **40**(3), 502–510
14. Yasuo, U.: The hand—Its Function and Anatomy, 4th edn. Kinpodo, Kyoto (2006). (in Japanese)
15. Kyozo, Y., Shigenobu, I., Toru, K.: Joint range of motion display and measurement method. Japn. J. Rehabil. Med. **32**(4), 207–217 (1995) (in Japanese) (http://doi.org/10.2490/jjrm1963.32.207)